JACS
JOURNAL OF THE AMERICAN CHEMICAL SOCIETY
Communication
pubs.acs.org/JACS

# Ultrathin Icosahedral Pt-Enriched Nanocage with Excellent Oxygen Reduction Reaction Activity

Dong Sheng He,[†,∥] Daping He,[†,∥] Jing Wang,[†] Yue Lin,[‡] Peiqun Yin,[†] Xun Hong,[†] Yuen Wu,*[,†] and Yadong Li*[,†,§]

[†]Center of Advanced Nanocatalysis, University of Science and Technology of China, Hefei, Anhui 230026, China

[‡]Hefei National Laboratory for Physical Sciences at the Microscale, University of Science and Technology of China, Hefei, Anhui Province 230026, P. R. China

[§]Department of Chemistry and Collaborative Innovation Center for Nanomaterial Science and Engineering, Tsinghua University, Beijing 100084, China

Supporting Information

**ABSTRACT:** Cost-efficient utilization of Pt in the oxygen reduction reaction (ORR) is of great importance for the potential industrial scale demand of proton-exchange membrane fuel cells. Designing a hollow structure of a Pt catalyst offers a great opportunity to enhance the electrocatalytic performance and maximize the use of precious Pt. Herein we report a routine to synthesize ultrathin icosahedral Pt-enriched nanocages. In detail, the Pt atoms were conformally deposited on the surface of Pd icosahedral seeds, followed by selective removal of the Pd core by a concentrated $HNO_3$ solution. The icosahedral Pt-enriched nanocage that is a few atomic layers thick includes the merits of abundant twin defects, an ultrahigh surface/volume ratio, and an ORR-favored Pt{111} facet, all of which have been demonstrated to be promoting factors for ORR. With a 10 times higher specific activity and 7 times higher mass activity, this catalyst shows more extraordinary ORR activity than the commercial Pt/C. The ORR activity of icosahedral Pt-enriched nanocages outperforms the cubic and octahedral nanocages reported in the literature, demonstrating the superiority of the icosahedral nanocage structure.

Proton-exchange membrane fuel cells are expected to be a promising nonpolluting technology for energy conversion.[1] As is well-known, this technology is constrained by the kinetically limited oxygen reduction reaction (ORR) at the cathode.[2] Pt-based catalysts are currently the most efficient materials in catalyzing the ORR.[3] However, the low abundance of Pt in the earth's crust, plus its high price, limits its broad and practical applications in fuel cells. For many years, various types of Pt-based nanoparticles have been synthesized in efforts to efficiently utilize Pt atoms in ORR. The geometrical and electrical structure of the Pt-based catalyst, which directly affects the adsorption of oxygen and its activation for ORR, is determined by the arrangement and configuration of the surface and/or topmost few layers of atoms.[4] It is reasonable to predict that the hollow or core−shell structures with a few layers of Pt atoms at the surface could serve as ideal model catalysts for the surface sensitive ORR.[5] Compared with core−shell structures, the hollow structures, such as the frame, cage, exhibit more fantastic potential by exposing the interior surface and three-dimensional molecular accessibility.[4] In addition, for ORR, Markovic and Ross pointed out that the specific activity of Pt{111} is at least twice that of Pt{100} in $HClO_4$ solution.[6] Recently, Xia's group also has demonstrated the Pt octahedral nanocage with {111} facets bounded is more active than the Pt cubic nanocage with {100} facets bounded.[4] Thus, Pt nanoparticles with a {111} bounded nanocage structure are expected to have good electrocatalytic activity toward ORR.

For the structure-sensitive reactions, introducing defects such as twin boundaries could apparently reduce the activation energy and further improve the catalytic process.[7] This turns our attention to the icosahedron, which has the most density of twins per particle in face centered metals. In fact, an icosahedron consists of 20 tetrahedra and each tetrahedron is adjacent to another with a twin boundary,[8] endowing the icosahedral nanocage as an ideal catalyst to further enhance the catalytic efficiency. Recently, both solid icosahedral Pt, Pt−Ni and core−shell Pd−Pt have been demonstrated to have superior electrocatalytic activity toward ORR because of the existence of a twin boundary.[3,9] However, due to increased surface strain derived from the high density of defects at twin boundaries, fabrication of the hollow Pt nanocage with icosahedral symmetry and a thickness of a few atomic layers is a great challenge. In this paper, taking the Pd icosahedron as the seed, we were able to conformally deposit a few layers of Pt atoms on the surface of Pd to form a Pd−Pt core−shell structure. Followed by selectively removing the Pd core, novel icosahedral Pt-enriched nanocages were successfully constructed. Owing to the abundant twin defects, ultrahigh surface/volume ratio, and ORR-favored Pt{111} facet, these icosahedral Pt-enriched nanocages show superior ORR catalytic activity (with a mass activity of 1.12 $A{\cdot}mg^{-1}$ and specific activity of 2.48 $mA{\cdot}cm^{-2}$) than previously reported single crystal nanocages (for the octahedral nanocage, the mass activity is 0.75 $A{\cdot}mg^{-1}$ and the specific activity is 1.98 $mA{\cdot}cm^{-2}$; for cubic nanocages, the mass activity is 0.38 $A{\cdot}mg^{-1}$ and the specific activity is 0.82 $mA{\cdot}cm^{-2}$).

**Received:** December 1, 2015
**Published:** January 25, 2016





DOI: 10.1021/jacs.5b12530
J. Am. Chem. Soc. 2016, 138, 1494−1497

Figure 1 schematically illustrates the synthetic strategy of ultrathin Pt-enriched icosahedral nanocages. First, Pd icosahedral nanoparticles with a narrow size distribution (15.4 ± 1.8 nm) were synthesized via a previously reported method.[10] Figure S1 is a closer look of the Pd icosahedral seeds using aberration corrected scanning transmission electron microscopy (STEM) with high angle annular dark field (HAADF) and bright field (BF) detectors. Most of the nanoparticles exhibit a hexagonal shape, indicating icosahedral nanoparticles along with a favorable ⟨111⟩ or ⟨211⟩ direction. Based on the TEM analysis, the yield of icosahedral nanoparticles is estimated to be over ∼90%. These Pd icosahedra were used as the starting seeds for further Pt deposition. Since Pd and Pt have moderate lattice mismatch, the growth of the Pt shell will follow in the epitaxial growth fashion. By accurately controlling the quantity of the Pt precursor, ultrathin layers of Pt were coated on the surface of Pd icosahedra by mild reducing condition. From the size measurement in Figure 1, the thickness of the Pt layer was estimated to be ∼1 nm. After immersing the nanoparticles into concentrated $HNO_3$ solution, most of the Pd cores were selectively removed, leaving empty Pt-enriched nanocages. X-ray diffraction (XRD) spectra in Figure S2 indicate the peaks shifted from Pd to Pt after Pt coating and became broader after the removal of Pd.

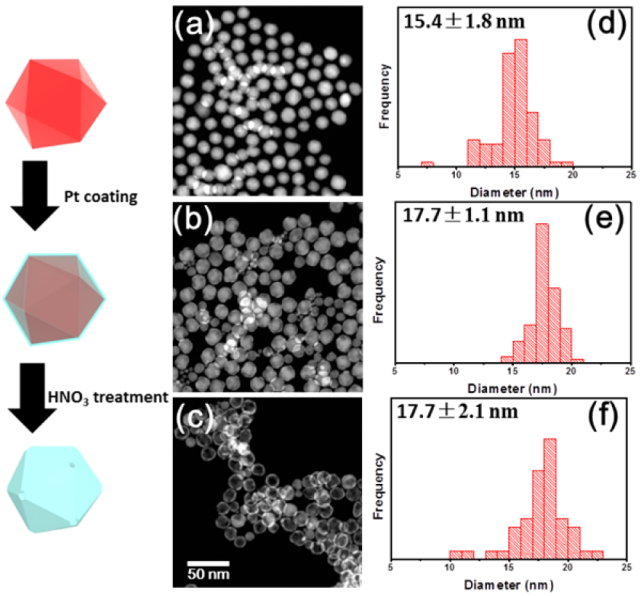


**Figure 1.** Left: Schematic illustration of the preparation of icosahedral Pt-enriched nanocages. (a) Pd icosahedral seeds. (b) Icosahedral Pd−Pt core−shell nanoparticles. (c) Icosahedral Pt-enriched nanocages. (a), (b) and (c) share the same scale bar in (c). (d), (e) and (f) are the size distributions of nanoparticles in (a), (b) and (c) respectively.

Figure 2 a and b are the HAADF and BF images of the Pd−Pt core−shell nanoparticle, respectively. In Figure 2b, the dark-bright contrast patterns of the inner part of the nanoparticles indicate that the core still remains as an icosahedral structure. Figure 2c and d are Pd and Pt signals from the Energy Dispersive X-ray (EDX) mapping of the Pd−Pt core−shell nanoparticles. It is very clear that Pd still remains in the center after the Pt coating and Pt atoms uniformly distributed around the core. Figure 2e is the enlarged HAADF-STEM image of the Pd−Pt interface. Thanks to the atomic contrast (Z contrast), the atomic arrangement of Pt and Pd, where Pt atoms are brighter than Pd atoms, can be clearly clarified. It shows that a few layers of Pt atoms epitaxially grew on the surface of Pd. This is also evidenced by the fast Fourier transform (FFT) in the inset of Figure 2e, where the FFT shows only one set of an fcc [011] diffractogram.

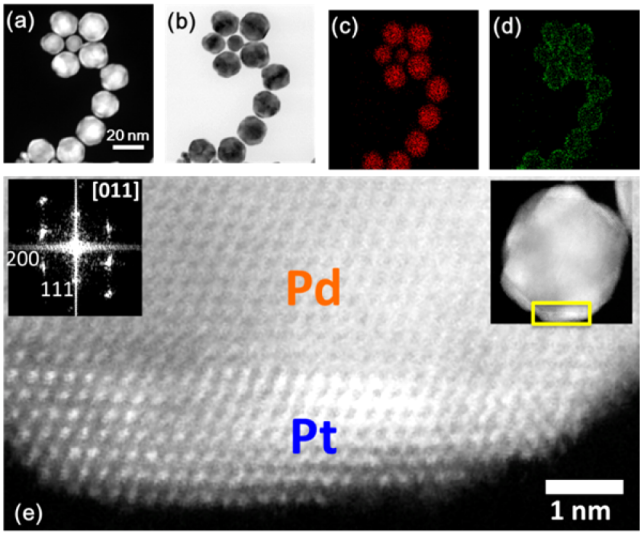


**Figure 2.** Simultaneously acquired (a) HAADF and (b) BF images of Pd−Pt core−shell nanoparticles. (c) Pd and (d) Pt signal of EDX mapping. (e) Atomically resolved HAADF-STEM image of Pd−Pt interface. Left inset is the FFT of (e). Right inset shows the interface at the low magnification.

Because of the interdiffusion and alloying of Pt and Pd, it is possible to form Pd channels in the Pt shells.[4] When these nanoparticles were immersed in concentrated $HNO_3$ solution, the Pd atoms were dissolved gradually from the surface to the inner part.[11] As shown in Figure 3a and b, the inner part of the nanoparticles became empty after the $HNO_3$ treatment, indicating the removal of Pd. In fact, through careful inspection of the ICP-MS measurement, trace Pd still remains (∼10 wt %) in the leaving residue.[11] This is in accordance with the fact that the Pd signals are found in EDX mapping at the sites of the shell of the nanocages (Figure 3c). Figure 3e is an atomic resolution HAADF-STEM image of a hollow Pt-enriched nanocage, which shows a characteristic lattice fringe of an icosahedron. For comparison, an atomic model and a kinematic HAADF-STEM simulation of a solid icosahedron nanoparticle are displayed in Figure 3f and g with 3-fold symmetry orientation.[12] The lattice fringes of both experimental and simulated images show a similar pattern, where the lattice lines go outward radically from the center with a 6-fold symmetry. The FFTs of both experimental (inset in Figure 3e) and simulated images (Figure 3h) are also similar.

The ORR measurement of the icosahedral Pt-enriched nanocage/C, Pd−Pt core−shell/C, and commercial Pt/C catalyst (JM) (20% by wt of ∼3 nm Pt nanoparticles on Vulcan XC-72 carbon) support is summarized in Figure 4. As shown in Figure 4a, the ORR polarization curves exhibit a positive shift in the following order: Pt/C < Pd−Pt core−shell/C < Pt-enriched nanocage/C. The kinetic current was calculated from the ORR polarization curve by the Koutecky−Levich equation,[13] with a decreased Tafel slope from 72 mV $dec^{-1}$ for Pt/C to 63 mV $dec^{-1}$ for Pt-enriched nanocage/C (Figure 4b). These results show that the Pt-enriched nanocage/C catalyst has the best kinetic behavior and


DOI: 10.1021/jacs.5b12530
J. Am. Chem. Soc. 2016, 138, 1494−1497

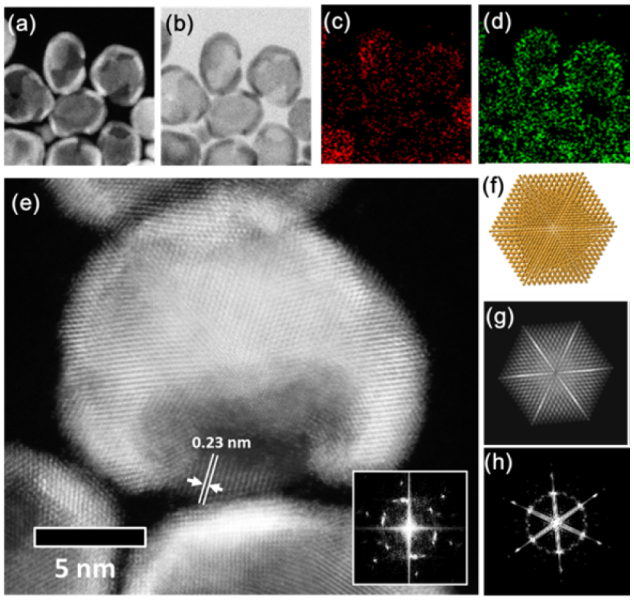


**Figure 3.** Simultaneously acquired (a) HAADF-STEM and (b) BF-STEM images of icosahedral-enriched nanocages. (c) Pd and (d) Pt signals of EDX mapping. (e) Atomically resolved HAADF-STEM image of an icosahedral Pt-enriched nanocage. The inset is the FFT of the image. (f) Atomic model of an icosahedral nanoparticle. (g) Kinematic STEM-HAADF simulation of the nanoparticle in (f) with the same direction. (h) FFT of the image in (g).

highest kinetic current density. Figure 4c illustrates cyclic voltammetry (CV) curves of different samples in nitrogen saturated 0.1 M $HClO_4$ solution between 0.05 and 1.25 V at a sweep rate of 50 mV $s^{-1}$. The specific electrochemical active surface area (ECSA) of the Pt-enriched nanocage/C, Pt−Pd core−shell/C, and Pt/C catalysts were calculated by measuring the charges collected in the hydrogen adsorption/desorption region (0.05−0.35 V) after double-layer correction and assuming for hydrogen monolayer adsorption as 210 $\mu$C $cm^2$.[14] As a result, the specific ECSA of the Pt enriched nanocage (45.0 $m^2$ $g^{-1}$ Pt) was found to be higher than that of the Pd−Pt core−shell/C catalyst (38.8 $m^2$ $g^{-1}$ Pt) due to the exposure of the interior surface.

The kinetic current was normalized to both the loading amount of metal and ECSA in order to compare the mass activity and special activity of different catalysts. As shown in Figure 4d, the Pt-enriched nanocage/C exhibits a mass activity of 1.12 A $mg^{-1}$ Pt at 0.9 V versus a reversible hydrogen electrode (RHE), which is ∼7 times greater than that of the commercial Pt/C catalyst (0.16 A $mg^{-1}$), and is ∼4 times greater than that of the Pd−Pt core−shell/C (0.29 A $mg^{-1}$) catalyst. The specific activity of Pt-enriched nanocage/C (2.48 mA $cm^{-2}$) is ∼10 times that of the Pt/C catalyst (0.25 mA $cm^{-2}$) and ∼3.5 times that of the Pd−Pt core−shell/C catalyst (0.74 mA $cm^{-2}$) at 0.9 V (Figure 4e). This catalyst outperforms the single crystal nanocages such as octahedral and cubic nanocages, which have a maximum performance that is 5 times higher in mass activity and 7 times higher in specific activity than commercial Pt/C. The stability of Pt-enriched nanocage/C was investigated by accelerated degradation testing, using linear potential sweeps during potential cycling between 0.6 and 1.0 V at 50 mV $s^{-1}$ in aqueous $O_2$-saturated 0.1 M $HClO_4$ solution (Figure 4f). After 10 000 cycles, the commercial Pt/C catalyst (inset of Figure 4f) showed an ∼36 mV degradation in

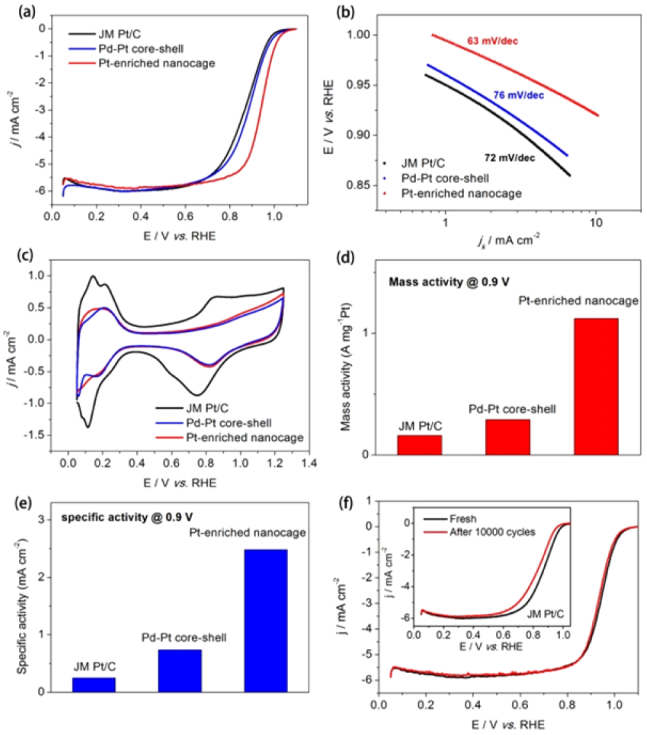


**Figure 4.** (a) ORR polarization curves. (b) The corresponding Tafel plots for Pt-enriched nanocage/C, Pd−Pt core−shell/C, and Pt/C in $O_2$-saturated 0.1 M $HClO_4$ solution with a sweep rate of 10 mV $s^{-1}$ and a rotation rate of 1600 rpm. The currents were normalized to the geometric area of the rotating disk electrode (0.196 $cm^2$). (c) Cyclic voltammetry curves of Pt-enriched nanocage/C, Pt−Pd core−shell/C, and Pt/C in N2-saturated 0.1 M $HClO_4$ solution at room temperature. (d) Mass activity for these three catalysts at 0.9 V versus RHE. (e) Specific activity at 0.9 V based on the ECSAs. (f) ORR polarization curves of Pt-enriched nanocage and Pt/C (inset figure) before and after 10 000 cycles.

half-wave potential and 50% decrease in mass activity, while the Pt-enriched nanocage/C showed nearly no degradation. In addition, electron micrographs in Figures S6 and S7 show that the icosahedral Pt-enriched nanocages maintained the hollow icosahedral shape after the accelerated degradation testing, rather than particle aggregation which is frequently observed in a commercial Pt/C sample.

To conclude, we have successfully deposited a few-layer-thick Pt shell on Pd to form icosahedral core−shell nanoparticles. Through selective etching of Pd, ultrathin Pt-enriched nanocages with icosahedral symmetry and {111} facets bounded were obtained. This icosahedral Pt nanocage showed extraordinary activity for ORR over Pd−Pt core−shell and commercial Pt/C, which may be attributed to the dense twin defects at the surface, exposure of the internal surface, and ORR-favorable Pt {111} facets. The icosahedral Pt-enriched nanocage is a very promising candidate structure for Pt-based ORR catalysts, whose activity may be further enhanced by alloying with 3d metals such as Fe, Co, and Ni.

## ■ ASSOCIATED CONTENT

### Supporting Information

The Supporting Information is available free of charge on the ACS Publications website at DOI: 10.1021/jacs.5b12530.

The detailed synthesis and characterization (PDF)



DOI: 10.1021/jacs.5b12530
J. Am. Chem. Soc. 2016, 138, 1494−1497

## AUTHOR INFORMATION


### Corresponding Authors

*yuenwu@ustc.edu.cn

*ydli@mail.tsinghua.edu.cn

### Author Contributions

‖D.S.H. and D.P.H. contributed equally.


### Notes

The authors declare no competing financial interest.

## ACKNOWLEDGMENTS

The authors would like to thank Dr. Chengming Wang for discussions in electrochemical measurement. D.S.H. would like to acknowledge the sponsorship of the Scientific Research Foundation for the Returned Overseas Scholars, Ministry of Education of China. This work was supported by the Fundamental Research Funds for the Central Universities (WK2060190043), National Natural Science Foundation of China (U1463202), State Key Project of Fundamental Research for Nanoscience and Nanotechnology (2011CB932401 and 2011CBA00500), and National key Basic Research Program of China (2012CB224802).

## REFERENCES


(1) (a) Nie, Y.; Li, L.; Wei, Z. *Chem. Soc. Rev.* **2015**, *44*, 2168. (b) Debe, M. K. *Nature* **2012**, *486*, 43. (c) Liu, Y.; Gokcen, D.; Bertocci, U.; Moffat, T. P. *Science* **2012**, *338*, 1327.

(2) (a) Huang, X.; Zhao, Z.; Cao, L.; Chen, Y.; Zhu, E.; Lin, Z.; Li, M.; Yan, A.; Zettl, A.; Wang, Y. M.; Duan, X.; Mueller, T.; Huang, Y. *Science* **2015**, *348*, 1230. (b) Chen, C.; Kang, Y.; Huo, Z.; Zhu, Z.; Huang, W.; Xin, H. L.; Snyder, J. D.; Li, D.; Herron, J. A.; Mavrikakis, M.; Chi, M.; More, K. L.; Li, Y.; Markovic, N. M.; Somorjai, G. A.; Yang, P.; Stamenkovic, V. R. *Science* **2014**, *343*, 1339.

(3) (a) Wang, X.; Choi, S. I.; Roling, L. T.; Luo, M.; Ma, C.; Zhang, L.; Chi, M.; Liu, J.; Xie, Z.; Herron, J. A.; Mavrikakis, M.; Xia, Y. *Nat. Commun.* **2015**, *6*, 7594. (b) Long, N. V.; Asaka, T.; Matsubara, T.; Nogami, M. *Acta Mater.* **2011**, *59*, 2901. (c) Choi, R.; Choi, S. I.; Choi, C. H.; Nam, K. M.; Woo, S. I.; Park, J. T.; Han, S. W. *Chem. - Eur. J.* **2013**, *19*, 8190. (d) Li, H. H.; Ma, S. Y.; Fu, Q. Q.; Liu, X. J.; Wu, L.; Yu, S. H. *J. Am. Chem. Soc.* **2015**, *137*, 7862. (e) Wang, X.; Vara, M.; Luo, M.; Huang, H.; Ruditskiy, A.; Park, J.; Bao, S.; Liu, J.; Howe, J.; Chi, M.; Xie, Z.; Xia, Y. *J. Am. Chem. Soc.* **2015**, *137*, 15036.

(4) Zhang, L.; Roling, L. T.; Wang, X.; Vara, M.; Chi, M.; Liu, J.; Choi, S. I.; Park, J.; Herron, J. A.; Xie, Z.; Mavrikakis, M.; Xia, Y. *Science* **2015**, *349*, 412.

(5) (a) Park, J.; Zhang, L.; Choi, S. I.; Roling, L. T.; Lu, N.; Herron, J. A.; Xie, S.; Wang, J. G.; Kim, M. J.; Mavrikakis, M.; Xia, Y. *ACS Nano* **2015**, *9*, 2635. (b) Xie, S.; Choi, S. I.; Lu, N.; Roling, L. T.; Herron, J. A.; Zhang, L.; Park, J.; Wang, J.; Kim, M. J.; Xie, Z.; Mavrikakis, M.; Xia, Y. *Nano Lett.* **2014**, *14*, 3570.

(6) Markovic, N. M.; Ross, P. N., Jr. *Surf. Sci. Rep.* **2002**, *45*, 117.

(7) (a) Quan, Z.; Wang, Y.; Fang, J. *Acc. Chem. Res.* **2013**, *46*, 191. (b) Zhang, L.; Niu, W.; Xu, G. *Nano Today* **2012**, *7*, 586. (c) Dahl, S.; Logadottir, A.; Egeberg, R. C.; Larsen, J. H.; Chorkendorff, I.; Törnqvist, E.; Nørskov, J. K. *Phys. Rev. Lett.* **1999**, *83*, 1814.

(8) Hofmeister, H. *Encyclopedia of Nanosci. and Nanotechnol.* **2003**, *3*, 431.

(9) (a) Zhou, W.; Wu, J.; Yang, H. *Nano Lett.* **2013**, *13*, 2870. (b) Wu, J.; Qi, L.; You, H.; Gross, A.; Li, J.; Yang, H. *J. Am. Chem. Soc.* **2012**, *134*, 11880.

(10) Lv, T.; Wang, Y.; Choi, S. I.; Chi, M.; Tao, J.; Pan, L.; Cheng; Huang, Z.; Zhu, Y.; Xia, Y. *ChemSusChem* **2013**, *6*, 1923.

(11) (a) Bai, S.; Wang, C.; Jiang, W.; Du, N.; Li, J.; Du, J.; Long, R.; Li, Z.; Xiong, Y. *Nano Res.* **2015**, *8*, 2789. (b) Wang, L.; Yamauchi, Y. *J. Am. Chem. Soc.* **2013**, *135*, 16762.

(12) He, D. S.; Li, Z. Y.; Yuan, J. *Micron* **2015**, *74*, 47.

(13) He, D. P.; Jiang, Y. L.; Lv, H. F.; Pan, M.; Mu, S. C. *Appl. Catal., B* **2013**, *132-133*, 379.

(14) Lim, B.; Jiang, M.; Camargo, P. H. C.; Cho, E. C.; Tao, J.; Lu, X.; Zhu, Y.; Xia, Y. *Science* **2009**, *324*, 1302.




DOI: 10.1021/jacs.5b12530
*J. Am. Chem. Soc.* 2016, 138, 1494−1497